Modelling Electron Spin Decoherence at Low Temperatures

Gordan Horvat, Marina Kveder, and Jiangyang You

Computational Chemistry Day 2022
Ruđer Bošković Institute
Zagreb, Croatia

September 24, 2022

- Supported by HRZZ projects IP-2013-11-1108 and IP-2018-01-3168.
- Based on G. Horvat, M. Kveder, JY, J. Eur. Phys. Plus 136 (2021) 842.
- See also JY, et. al., J. Chem. Phys. 150 (2019) 164124 and M. Kveder, B. Rakvin, JY, J. Chem. Phys. 151 (2019) 164124,
- as well as works from competitors: E. R. Canarie, S. M. Jahn, S. Stoll, J. Phys. Chem. Lett. 11 (2020) 3396, T. Bahrenberg, S. M. Jahn, A. Feintuch, S. Stoll, D. Goldfarb, Magn. Reson. 2 (2021) 161, and E. R. Canarie, S. M. Jahn, S. Stoll, J. Phys. Chem. Lett. 13 (2022) 5474.

Electron paramagnetic resonance (EPR)

- Measure the spectrum,

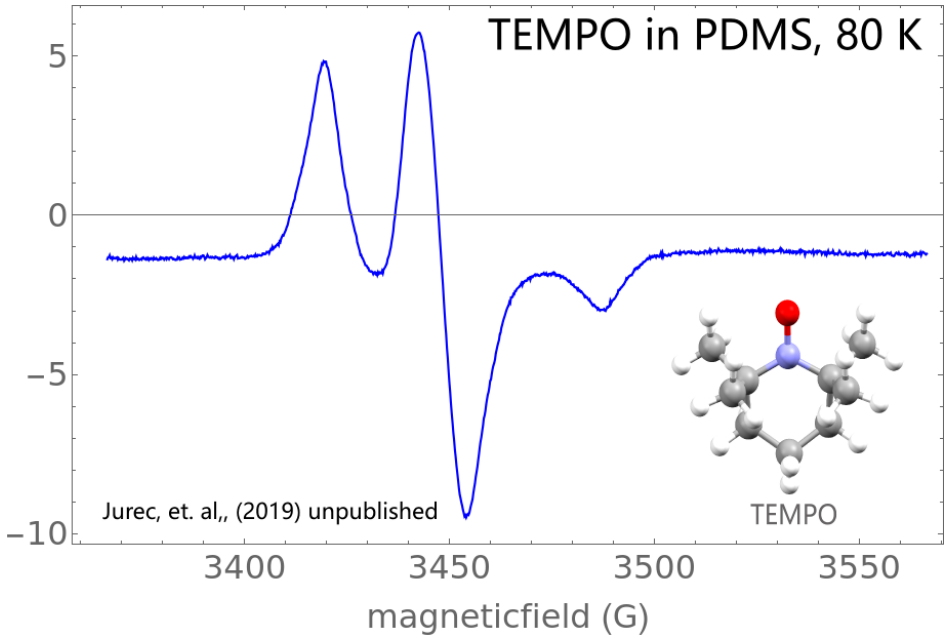

Electron paramagnetic resonance (EPR)

- Measure the spectrum, fit the spectrum,

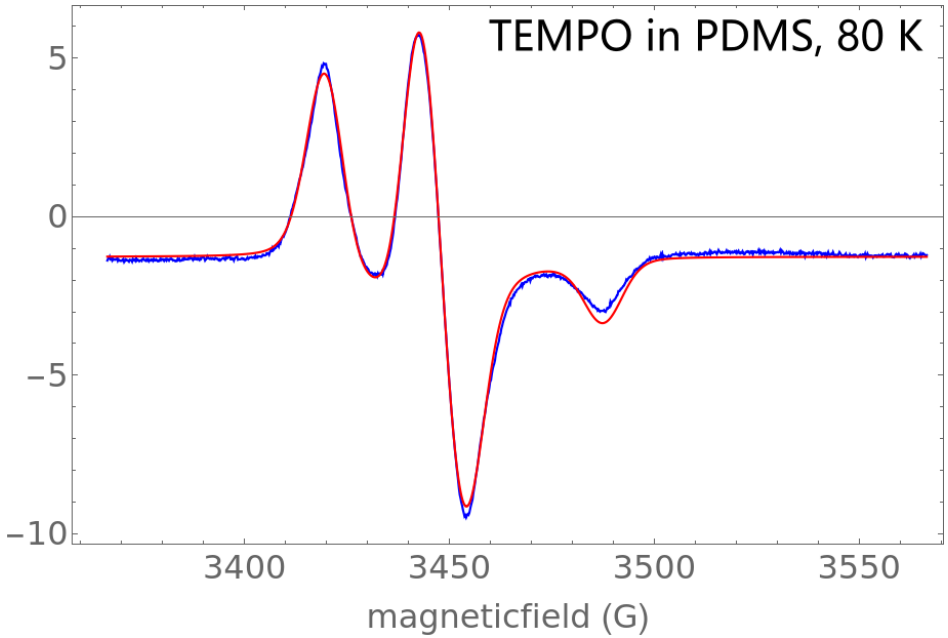

Electron paramagnetic resonance (EPR)

- Measure the spectrum, fit the spectrum,

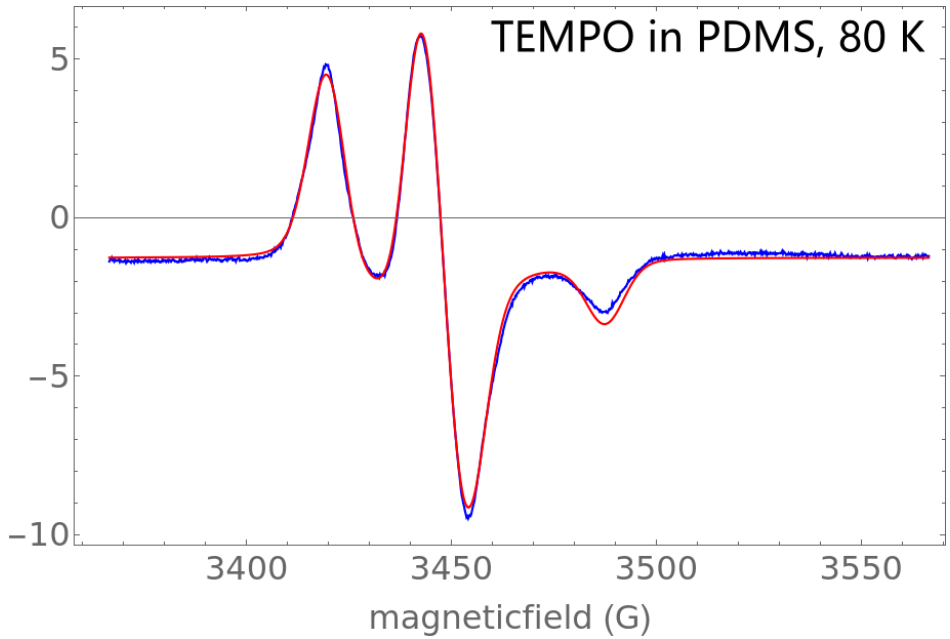

- Obtain parameters,

$$H_S = \mu_B \left(g_{xx} B_x S_x + g_{yy} B_y S_y + g_{zz} B_z S_z\right) + A_{xx} S_x I_x + A_{yy} S_y I_y + A_{zz} S_z I_z,$$

$$g_{xx} = 2.0090, g_{yy} = 2.0073, g_{zz} = 2.0024,$$

$$A_{xx} = 21.1 MHz, A_{yy} = 8.8 MHz., A_{zz} = 94.4 MHz.$$

Electron paramagnetic resonance (EPR)

- Measure the spectrum, fit the spectrum,

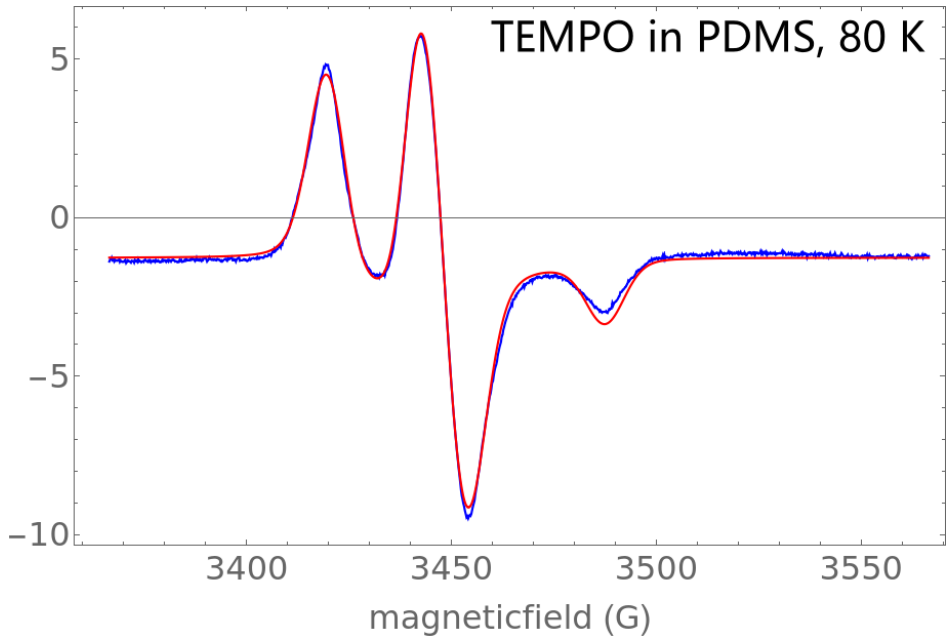

- Obtain parameters,

$$H_S = \mu_B \left(g_{xx} B_x S_x + g_{yy} B_y S_y + g_{zz} B_z S_z\right) + A_{xx} S_x I_x + A_{yy} S_y I_y + A_{zz} S_z I_z,$$

$$g_{xx} = 2.0090, g_{yy} = 2.0073, g_{zz} = 2.0024,$$

$$A_{xx} = 21.1 MHz, A_{yy} = 8.8 MHz., A_{zz} = 94.4 MHz.$$

- Wait for computational support.

Electron spin echo envelope decay and modulation

- Decay and modulation occurs in EPR Hahn echo experiments.

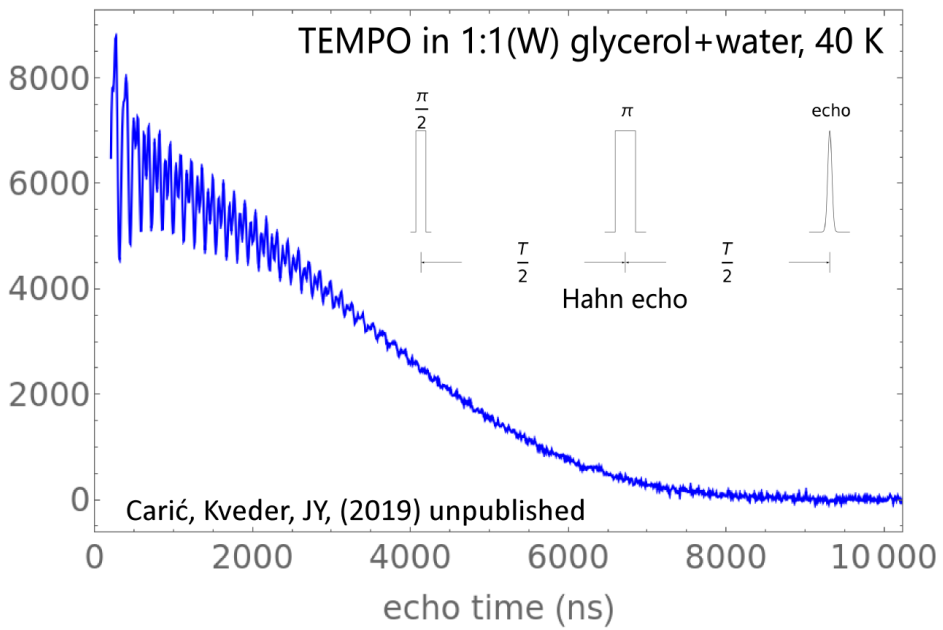

Electron spin echo envelope decay and modulation

- Decay and modulation occurs in EPR Hahn echo experiments.

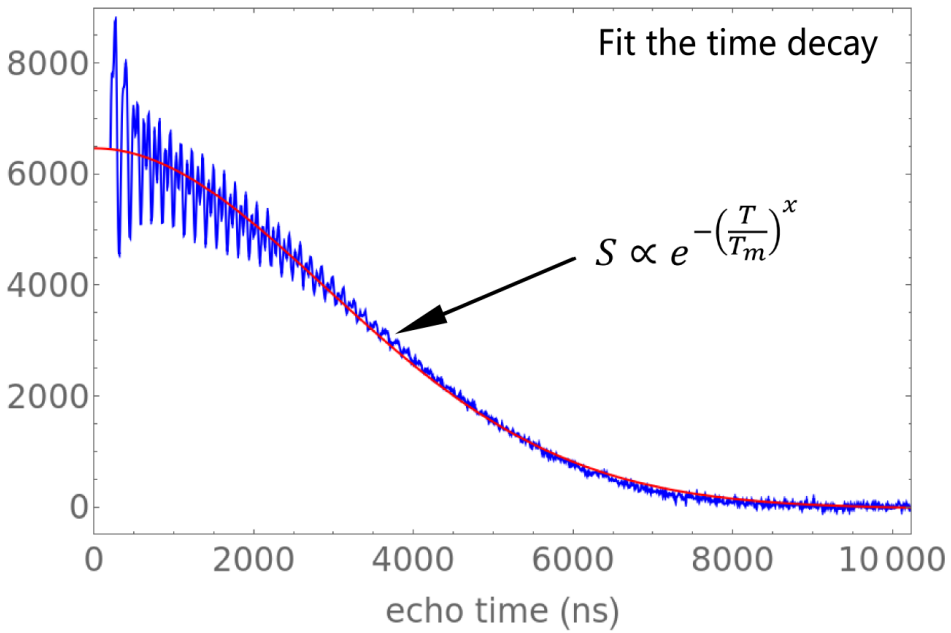

Electron spin echo envelope decay and modulation

- Decay and modulation occurs in EPR Hahn echo experiments.

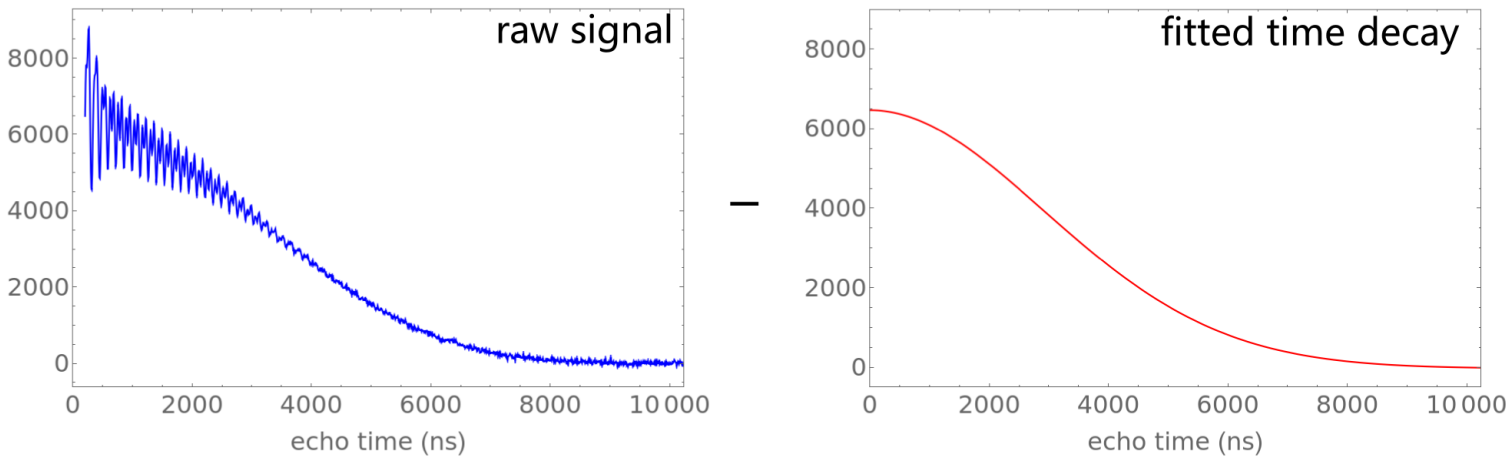

Electron spin echo envelope decay and modulation

- Decay and modulation occurs in EPR Hahn echo experiments.

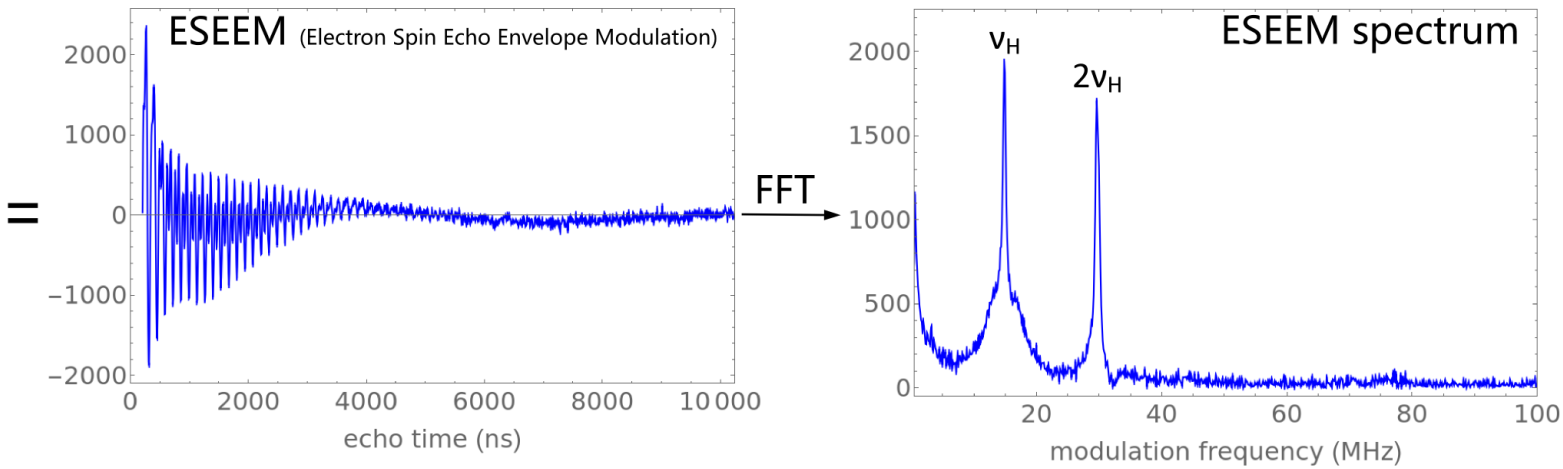

Electron spin echo envelope decay and modulation

- Decay and modulation occurs in EPR Hahn echo experiments.

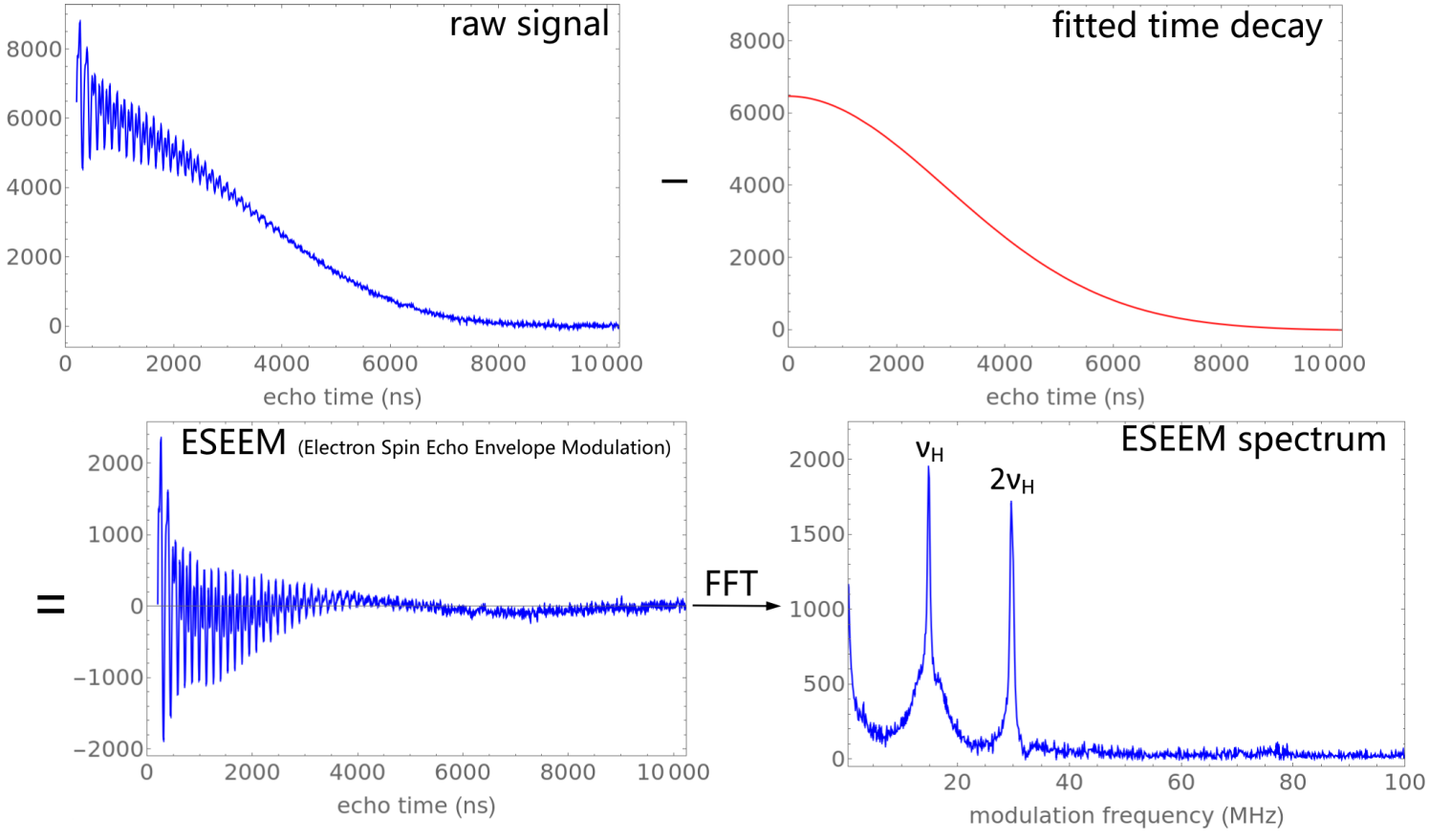

- Time decay controls the seeing into low frequency/long distance information. Hahn echo serves as a benchmark for more sophisticated experiments like double electron-electron resonance (DEER).

Electron spin echo envelope decay and modulation

- Decay and modulation occurs in EPR Hahn echo experiments.

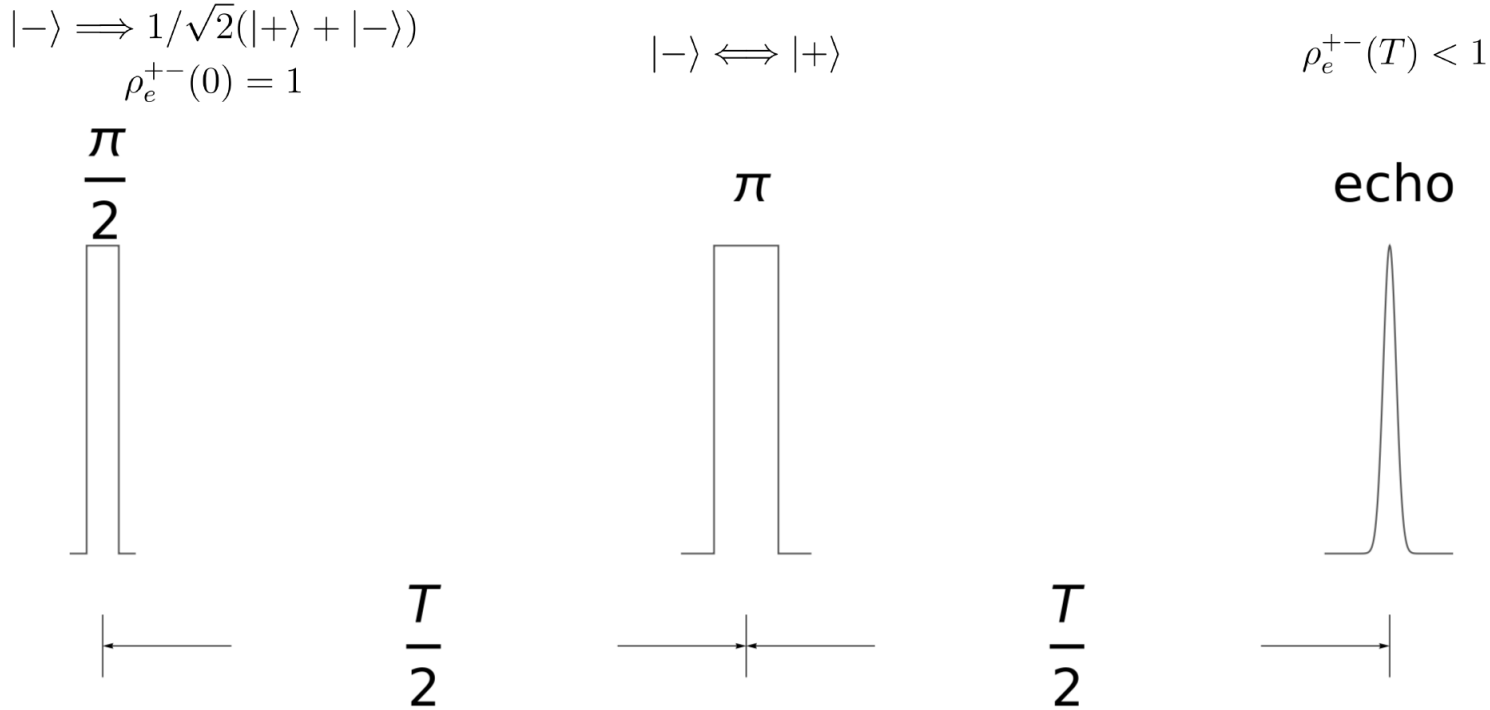

- Echo is proportional to remaining off-diagonal coherence $\mathcal{L}(t)$ of the initial electron spin state at the echo time T.

$$\mathcal{L}(t) \propto |\langle S^-(T)\rangle| = |\langle \rho_e^{+-}(T)\rangle|.$$

Electron spin echo envelope decay and modulation

- Predicting the time decay is desired and the focus of our work.

Extensions of Hahn echo

- Hahn echo can be extended by adding subsequent refocusing π-pulses.

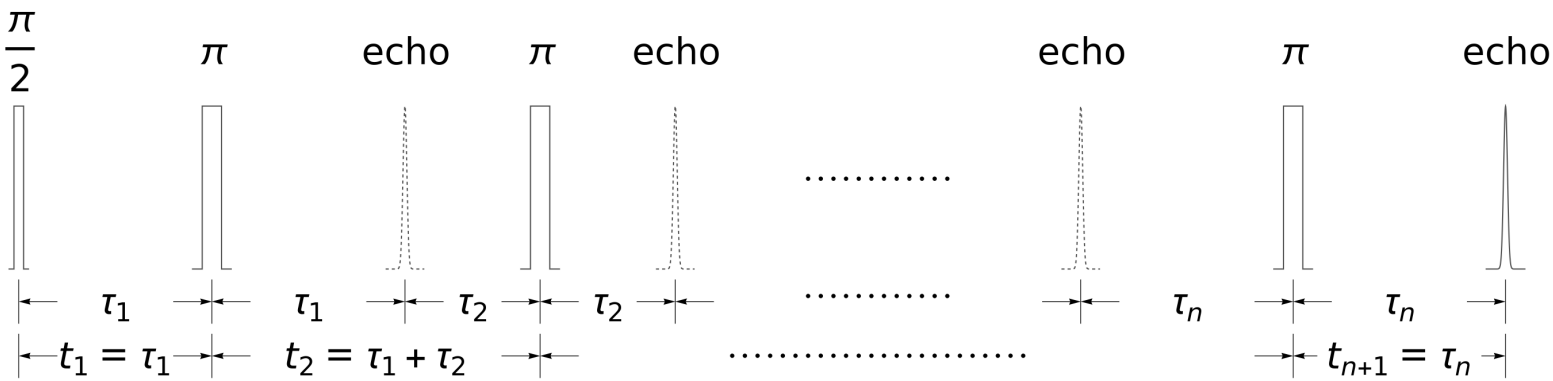

- Special examples are the Carr-Purcell and Uhrig dynamical decoupling (CPDD& UDD) pulse sequence series.

$$\mathrm{CPDD-n} \quad t_1 = t_{n+1} = \frac{T}{2n},\ t_2 = \ldots = t_n = \frac{T}{n},$$

$$\mathrm{UDD-n:} \quad T_k = \sum_{i=1}^{k} t_i = \frac{T}{2}\left(1 - \cos\frac{k\pi}{n+1}\right).$$

- DD preserve more coherence at equal echo time than Hahn echo, try to predict their time decays too.

The nuclear spin bath model

- Proposed for spin based quantum computing (W. Yao, R.-B. Liu, L.-J. Sham, PRB 74 (2006) 195301.), working on the isolated spin limit (radical concentration $<50\mu\mathrm{M}$).
- Decoherence due to large number of nuclear spin around, $N \simeq 500 \sim 2000$ in our work.
- Nuclear spins are frozen in space, only static spin-spin interactions matter.
- Only secular spin-spin couplings ($S^z I_i^z$, I_i^z, I_j^z, $I_i^+ I_j^- + I_i^- I_j^+$) are counted, works nicely for long time part of the decay.
- Calculate $\langle S^-(T)\rangle$ as bifringent evolution driven by $S^z \to \pm 1/2$, similar to modulation (Mims PRB 5 (1972) 2409).

$$\mathcal{L}_{\mathrm{Hahn}}(t) = \left|\langle\mathcal{I}| U_-(T/2)^\dagger U_+(T/2)^\dagger U_-(T/2) U_+(T/2) |\mathcal{I}\rangle\right|$$

- A 2^N dimensional linear algebra problem.

Cluster correlation expansion

- Decompose the 2^N dimensional matrix algebra into product of all the subclusters with increasing sizes. (W.Yang. R.-B. Liu, PRB 78 (2008) 085315)

$$\mathcal{L}(t) = \prod_{\{C\}} \mathcal{L}_C(t).$$

- Big cluster contributions have sub-cluster contributions removed, overcounting avoided.

$$\mathcal{L}_C(t) = \frac{\hat{\mathcal{L}}_C(t)}{\prod_{C' \subset C} \mathcal{L}_{C'}(t)}.$$

- Clusters with four protons often good enough, six-proton clusters were used for methyl group tunneling. (JCP 151 (2019) 164124)
- We rank the relevance of the cluster by the smallest proton pair dipolar coupling, $\lesssim 10^7$ clusters of four protons in total are affordable on good desktop computers.

Prepare the nuclear spin bath

- Need realistic distributions of protons, worked on crystals first for this reason. (JCP 150 (2019) 164124&151 (2019) 164124)
- Experiments are usually in glass matrices, make glass by MD.
- Learned simulated annealing in CCD 2018. (Vučemilović-Alagić, et. al., J. Colloid Interface Sci. 553 (2019) 350)

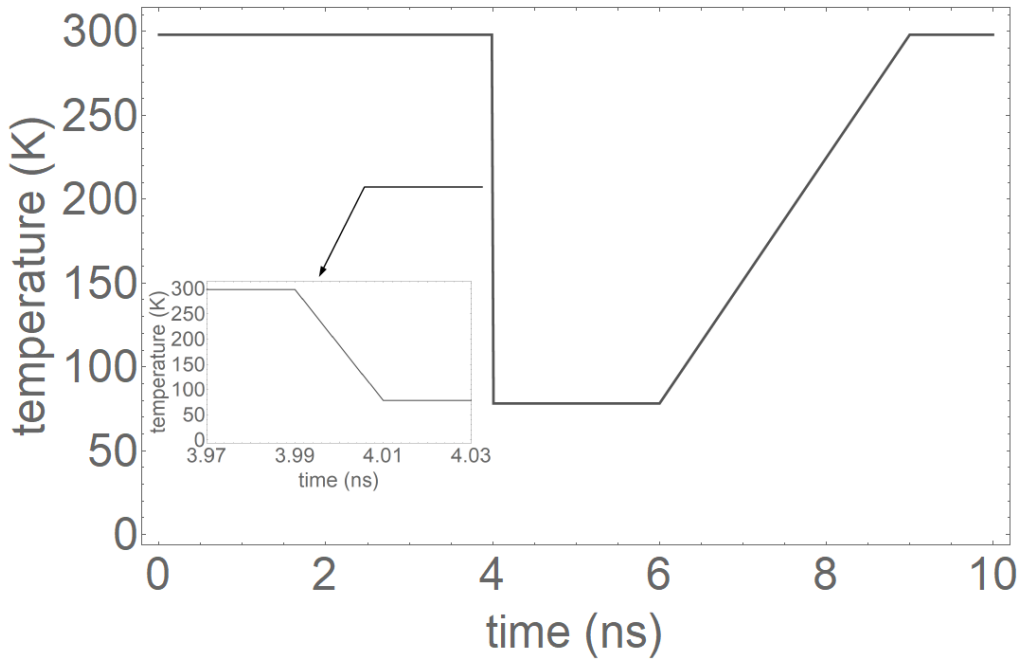

- 8∼16 periodic cycles, pick snapshots randomly from each 80K interval as glass structures, consistency self-tested.

The Hahn echo time decay

- Computed Hahn echo time decay profile of TEMPO in 1:1 (W) glycerol+water matrix was used to fit the actual experiment.

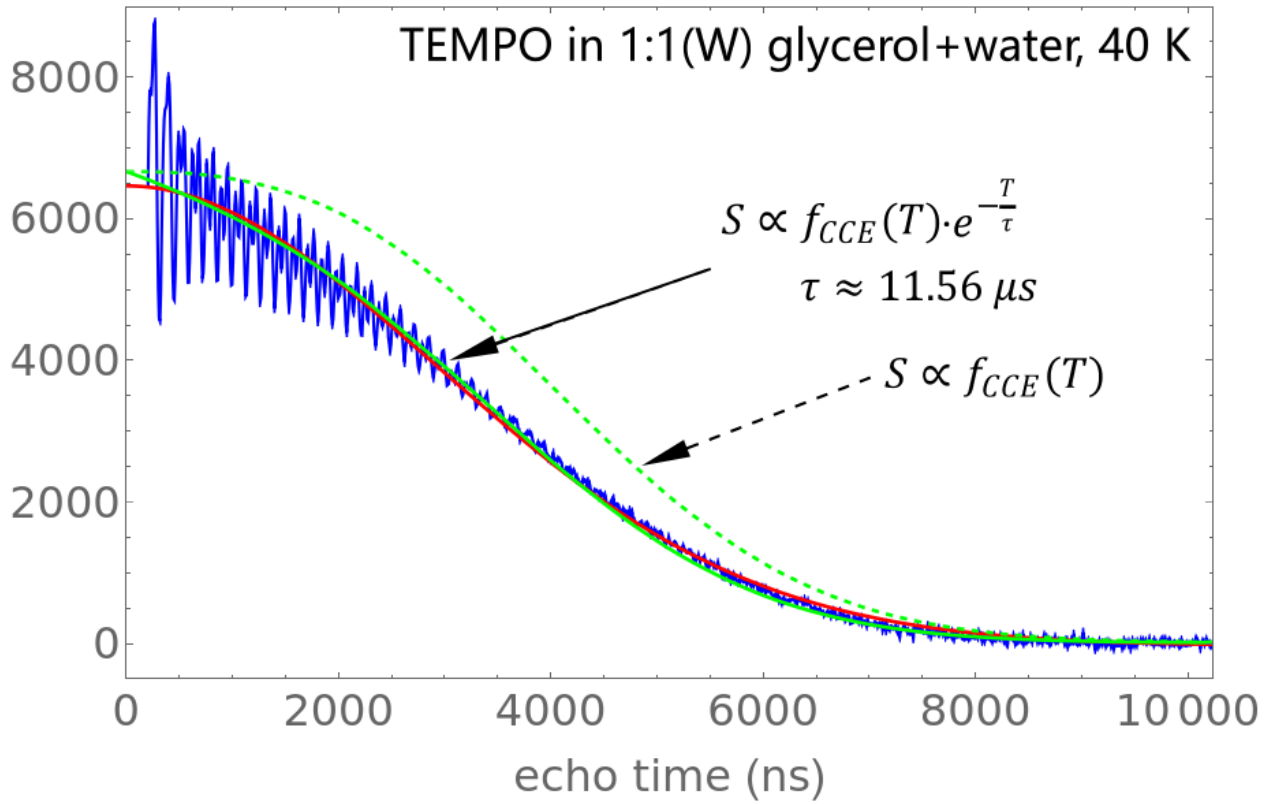

The Hahn echo time decay

- Computed Hahn echo time decay profile of TEMPO in 1:1 (W) glycerol+water matrix was used to fit the actual experiment.

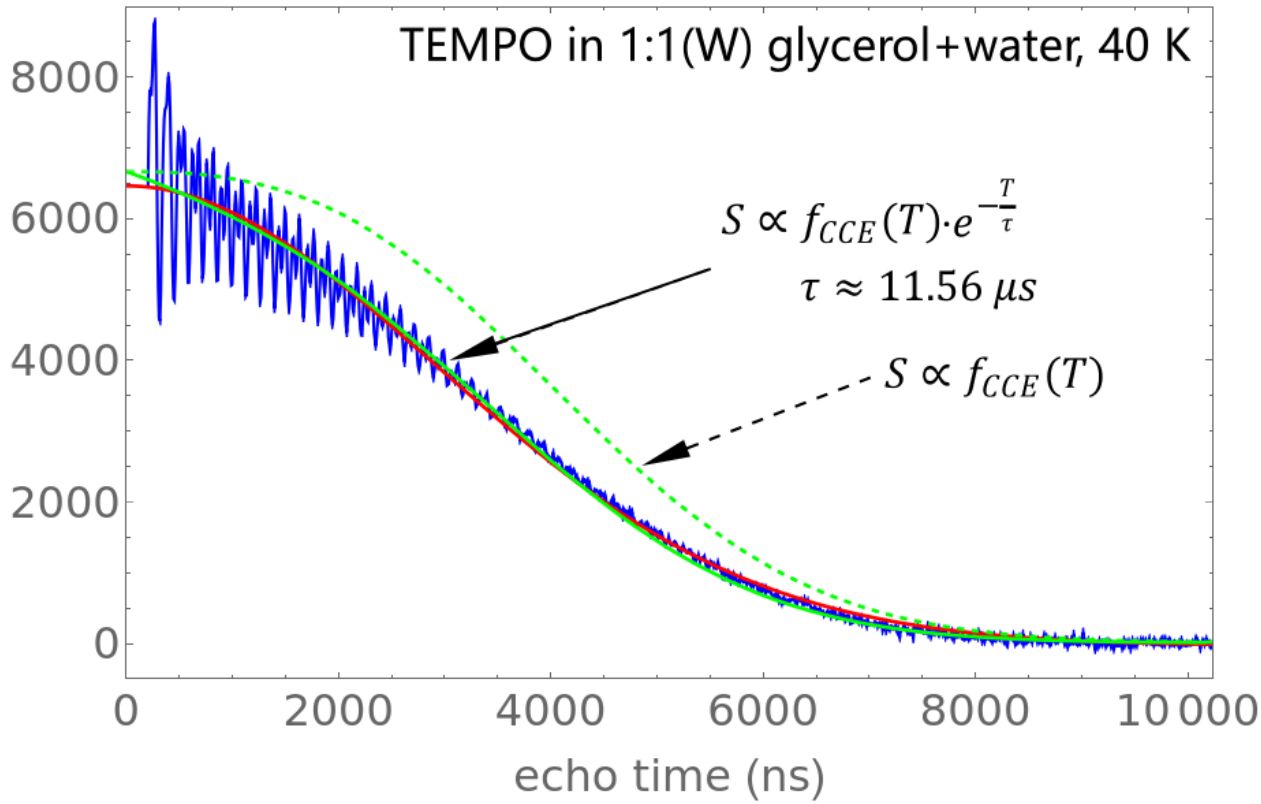

- Need additional corrections to match exactly CCE output with uncontrolled experiments. Competitor published similar results ahead of us.(Canarie, Jahn, Stoll, JPCL 11 (2020) 3396)

Comparison with DD experiments

- Our results compared favorably with controlled experiments.
  (Soetbeer, et. al., PCCP 20 (2018) 1615& 23 (2021) 5352)

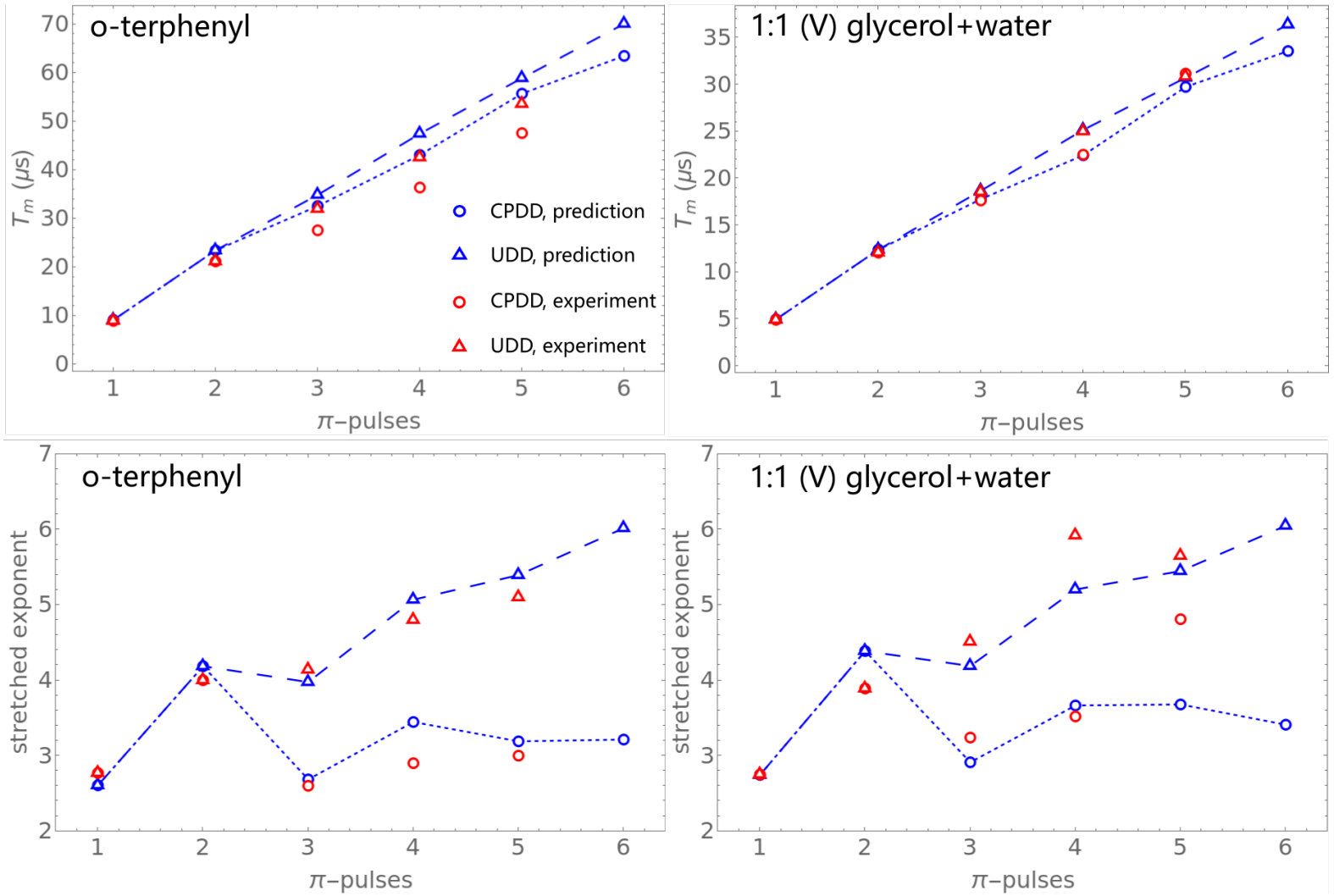

Interpulse interval variations

- Vary the interpulse interval ratios of symmetric ($t_i = t_{n-i+2}$) multiple spin echo pulse sequences. DD-1 and DD-2 are completely fixed by symmetry and echo forming conditions.

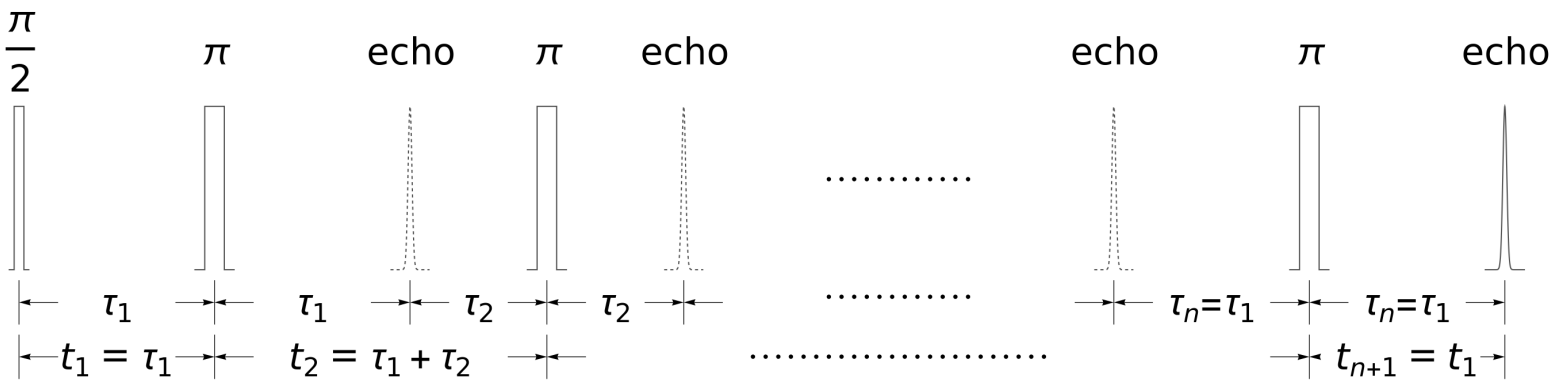

- All sequences with up to two ratio parameters (DD-3 to DD-6) were studied.

$$\{t_i\}_{\mathrm{DD-3}} = \left\{\frac{\lambda}{6}T,\ \left(\frac{1}{2}-\frac{\lambda}{6}\right)T, \left(\frac{1}{2}-\frac{\lambda}{6}\right)T,\ \frac{\lambda}{6}T\right\},$$

$$\{t_i\}_{\mathrm{DD-4}} = \left\{\frac{\lambda}{8}T,\ \frac{T}{4},\ \left(\frac{1}{2}-\frac{\lambda}{4}\right)T, \frac{T}{4},\ \frac{\lambda}{8}T\right\},$$

$$\{t_i\}_{\mathrm{DD-5}} = \left\{\frac{\lambda\cdot T}{10}, \frac{\lambda+\delta}{10}T, \frac{5-2\lambda-\delta}{10}T, \frac{5-2\lambda-\delta}{10}T, \frac{\lambda+\delta}{10}T, \frac{\lambda\cdot T}{10}\right\},$$

$$\{t_i\}_{\mathrm{DD-6}} = \left\{\frac{\lambda\cdot T}{12}, \frac{\lambda+\delta}{12}T, \frac{3-\lambda}{12}T, \frac{3-\lambda-\delta}{6}T, \frac{3-\lambda-\delta}{6}T, \frac{3-\lambda}{12}T, \frac{\lambda+\delta}{12}T, \frac{\lambda\cdot T}{12}\right\}.$$

Optimized DD pulse sequences

- DD-3∼6 can be moderately optimized.

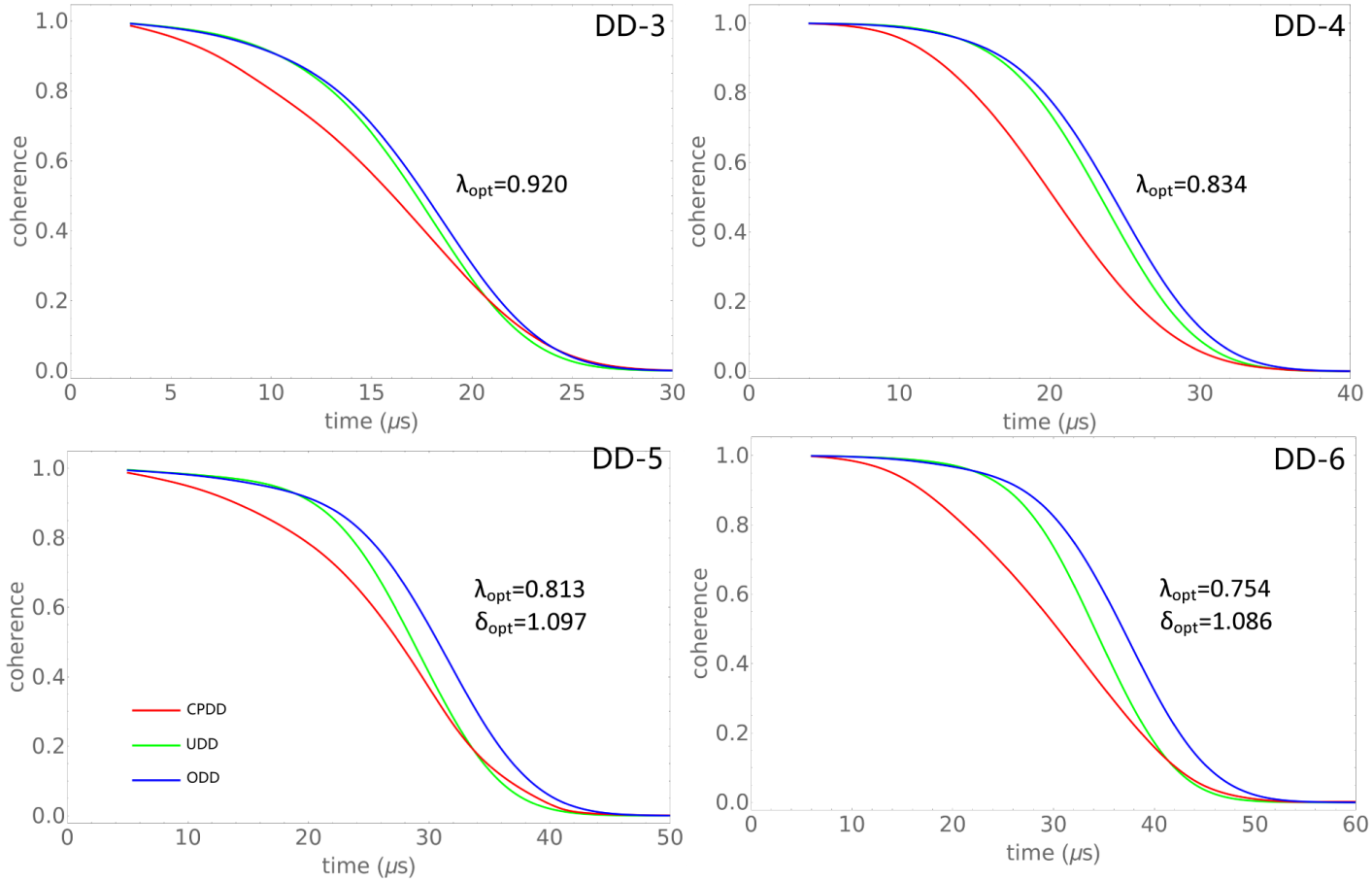

- Competitors found a nicer application in DEER by asymmetrizing DD-2.(Bahrenberg, et. al., Magn. Reson. 2 (2021) 161)

Summary

- In past,
  - Long time electron spin decoherence under Hahn echo and generalizations at low temperatures are calculated.
  - Molecular dynamics generated adequate structure inputs for the nuclear spin bath model.
  - Results compare favorably with experiments available in literature.
  - Competitors published higher profitable results ahead of us repeatedly.
- In future,
  - A few follow-up problems: more pulse sequences, including modulation, including dynamical effects like methyl group tunneling, etc..
  - Competitors will keep cleaning up the current field.

Outlook

- My EPR wishlist for computational chemists:
  - Spin Hamiltonian parameters for predicting spectra of (arbitrary) spin-1/2 paramagnetic centers.
  - Spin self-interaction ("zero field splitting"). ORCA could do quadratic terms, quartic needed for spin-5/2 particles (Mn^{2+}, Fe^{3+}), hexatic for lanthanides.
  - I need good methods to estimate torsion potentials of hindered methyl groups in order to calculate their impacts on ESEEM.
  - .....

Outlook

- Use G16 and keyword “NMR” for free radical spin Hamiltonian parameters. “property=EPR” won’t compute the g-tensor.

Thank you.

Solvents	box filling	temperature	density, MD	density, exp.
glycerol	1000	298.15 K	1.216 g/ml	1.258 g/m
glycerol/TIP3 1:1 (M)	960/960	298.15 K	1.184 g/ml	1.205 g/ml
glycerol/TIP3 1:1 (V)	379/1537	298.15 K	1.125 g/ml	1.140 g/ml
glycerol/TIP3 1:1 (W)	332/1698	298.15 K	1.113 g/ml	1.124 g/ml
tetrahydrofuran	1000	298.15 K	0.902 g/ml	0.889 g/ml
t-decalin	1000	298.15 K	0.870 g/ml	0.866 g/ml
bezene	1000	298.15 K	0.863 g/ml	0.871 g/ml
o-terphenyl	1000	343.15 K	1.015 g/ml	1.044 g/m
		220 K	1.075 g/ml	1.127 g/ml
phenyl salicylate	1000	333.15 K	1.133 g/ml	1.176 g/ml
		295 K	1.167 g/ml	1.202 g/ml

Table: Densities of the solvent boxes v.s. actual measurements.

	theory		experiment	
solvents	T_m (μs)	x	T_m (μs)	x
glycerol	5.75	2.62	5.2	2.4
glycerol/H_2O 1:1 (M)	5.33	2.70		
glycerol/H_2O 1:1 (V)	4.97	2.74	4.6 4.9	2.3 2.75
glyceroll/H_2O 1:1 (W)	4.83	2.63	4.33	2.77
tetrahydrofuran	5.15	2.70		
t-decalin	5.08	2.69		
decalin			4.2	2.1
benzene	7.95	2.59		
o-terphenyl	9.15	2.61	8.5 8.95	2.5 2.77
phenyl salicylate	10.34	2.57		

Table: Stretched exponential fit parameters of the Hahn echo decay of nitroxyl radicals embedded in several fast frozen solvent matrices.

Interval	T_m (μs)	σ_{T_m} (μs)	x	σ_x
1	9.18	0.22	2.61	0.09
2	9.05	0.23	2.55	0.09
3	9.30	0.26	2.63	0.11
4	9.17	0.20	2.56	0.10
5	8.98	0.22	2.66	0.09
6	9.07	0.24	2.60	0.11
7	9.08	0.20	2.58	0.09
8	9.10	0.21	2.59	0.10
"all"	9.12	0.24	2.60	0.10
"average'	9.12	0.07	2.59	0.04
OTP	9.15	0.24	2.62	0.11

Table: Average T_m and x, as well as their standard deviations σ_{T_m} and σ_x, obtained from reorientations of one MD snapshot from each of the periodic SA intervals 1-8 and their comparison versus random selections over all intervals.

	OTP matrix				1:1 (V) glycerol/H_2O matrix			
	theory		experiment		theory		experiment	
DD	T_m (μs)	x	T_m (μs)	x	T_m (μs)	x	T_m (μs)	x
DD1	9.15	2.61	8.95	2.77	4.97	2.74	4.92	2.75
DD2	23.47	4.19	21.2	4.0	12.40	4.39	12.08	3.89
CP3	32.59	2.68	27.6	2.6	17.77	2.91	17.64	3.24
U3	34.89	3.98	32.0	4.1	18.68	4.19	18.55	4.51
CP4	43.10	3.45	36.4	2.9	22.45	3.67	22.52	3.52
U4	47.48	5.07	43.6	4.8	25.16	5.20	25.00	5.92
CP5	55.73	3.19	47.6	3.0	29.74	3.68	31.16	4.81
U5	58.92	5.39	53.6	5.1	30.72	5.45	30.85	5.65
CP6	63.49	3.21			33.56	3.41		
U6	70.09	6.02			36.38	6.05		

Table: Comparison between the computational and experimental results of the decoherence of nitroxyl radical electron spin embedded in OTP and 1:1 (V) glycerol/H_2O mixture matrices.

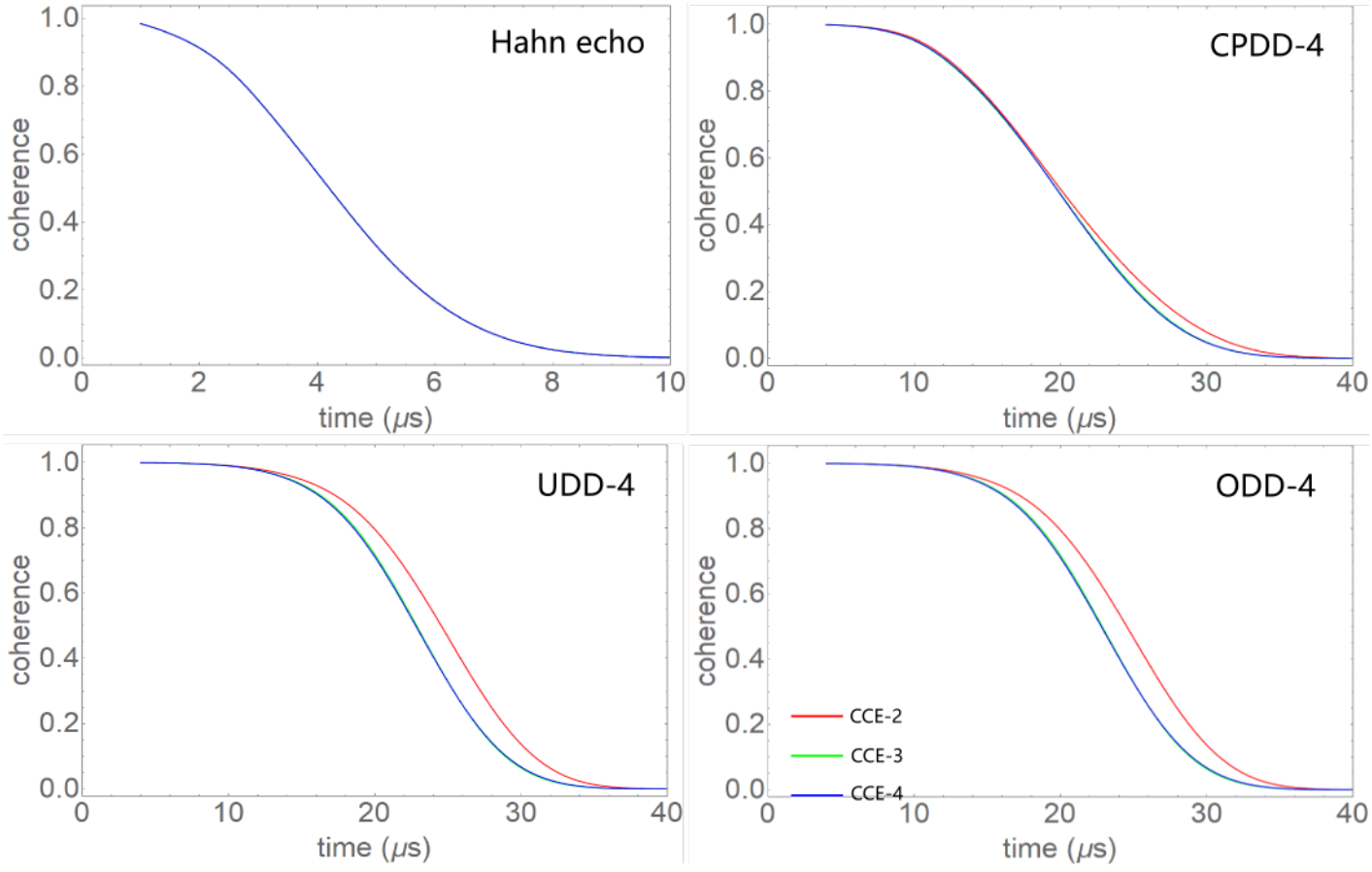

Figure: Contribution from clusters of different sizes to decoherence under different DD pulse sequences.

A_{iso} (G)	B3LYP		M062X		EPR
radical	Def2QZVPP	EPR-III	Def2QZVPP	EPR-III	experiment
TEMPONE	12.7	12.6	15.2	16.6	14.3
PYMeOH	9.9	9.9	12.1	13.6	14.3

Table: Isotropic hyperfine coupling of the radical $^{14}\mathrm{N}$ atom in two nitroxyl radicals TEMPONE and PYMeOH.